



## OPEN

# Intravital Microscopic Interrogation of Peripheral Taste Sensation

SUBJECT AREAS:  
OPTICAL IMAGING  
BIOPHOTONICS

Myunghwan Choi<sup>1,2</sup>, Woei Ming Lee<sup>1,3</sup> & Seok Hyun Yun<sup>1</sup>

<sup>1</sup>Harvard Medical School and Wellman Center for Photomedicine, Massachusetts General Hospital, 65 Landsdowne St., UP-5, Cambridge, Massachusetts 02139, USA, <sup>2</sup>Global Biomedical Engineering, Sungkyunkwan University, 2066 Seobu-ro, Jangan-Gu, Suwon, South Korea, <sup>3</sup>Research School of Engineering, Australian National University, Ian Ross Building, North Road, Canberra ACT 0200, Australia.

Received  
21 October 2014

Accepted  
12 January 2015

Published  
2 March 2015

Correspondence and  
requests for materials  
should be addressed to  
S.H.Y. (syun@mgh.  
harvard.edu)

**Intravital microscopy is a powerful tool in neuroscience but has not been adapted to the taste sensory organ due to anatomical constraint. Here we developed an imaging window to facilitate microscopic access to the murine tongue *in vivo*. Real-time two-photon microscopy allowed the visualization of three-dimensional microanatomy of the intact tongue mucosa and functional activity of taste cells in response to topically administered tastants in live mice. Video microscopy also showed the calcium activity of taste cells elicited by small-sized tastants in the blood circulation. Molecular kinetic analysis suggested that intravascular taste sensation takes place at the microvilli on the apical side of taste cells after diffusion of the molecules through the pericellular capillaries and tight junctions in the taste bud. Our results demonstrate the capabilities and utilities of the new tool for taste research *in vivo*.**

In vertebrates, the sense of taste in the tongue is mediated by specialized sensory cells genetically tuned to distinct taste qualities, such as sweet, salty, sour, bitter, and umami<sup>1</sup>. In response to chemical cues in the saliva, the taste cells elicit intracellular signals that are transmitted to the gustatory nerves and to the brain<sup>2</sup>. There exists intercellular communication among taste cells within a taste bud<sup>3,4</sup>. Taste sensation is further influenced by multisensory integration with olfactory input<sup>5</sup> and systemic modulation by blood-borne factors<sup>6</sup>.

Given the complex signaling crosstalks along with fragility of the cellular niche, a number of experimental tools have been established to investigate taste transduction pathway in living animals. Cognitive status such as food preference or avoidance is examined by behavioral assays, for example, by quantifying licking frequency to a certain food<sup>7</sup>. Functional cellular activity is commonly measured with direct electrical recording. Electrophysiology provides sensitive detection of electrical activity of nerves and neurons at single-spike resolution, but it requires invasive physical contact of an electrode with the cells and often lacks spatial information<sup>8</sup>. Recently, intravital fluorescence microscopy combined with chemical and genetic calcium probes has gained significant popularity due to its ability to detect cellular activity at high spatiotemporal resolution<sup>9</sup>. Functional calcium imaging in the gustatory cortex has been used to identify receptive fields for the basic taste qualities<sup>10</sup>. In the periphery, however, optical imaging has only been applied to *ex vivo* studies with isolated lingual epithelium or lingual slices<sup>11,12</sup>. Intravital microscopy has been successfully adapted to a variety of organs<sup>13–17</sup>, but the tongue poses a significant technical challenge due to its anatomical constraints. In the natural state, the tongue is positioned inside the oral cavity, which makes it inaccessible by conventional microscopy. In addition, functional calcium imaging requires mechanical stabilization of the tissue at a subcellular scale, which is difficult to achieve in the tongue *in vivo* due to physiologic respiratory and cardiac motions.

Here, we report cellular imaging of the dorsal surface of the tongue in live mice, for the first time to our knowledge. This was made possible by using a custom-made suction holder that externalizes the tongue from the oral cavity noninvasively and a tongue stabilizer that suppresses the tissue motion while allowing optical and chemical access simultaneously. Using these tools in combination with a video-rate two-photon microscope, we investigated the 3-dimensional structure and physiological calcium activity of taste cells in response to tastants that are administered orally or intravenously.

## Results

**Setup for Live Imaging of the Mouse Tongue.** We fabricated a miniature suction tip to grab and pull the tongue out of the oral cavity in a mouse under anesthesia (Fig. 1a, b and Supplementary Fig. S1). The suction tube had a rubber tip with an inner diameter of 1.5 mm. A suction pressure of about 25 mmHg (0.6 g-force) was found to be adequate to hold the externalized mouse tongue reliably without inducing tissue damage even for over 30 min of

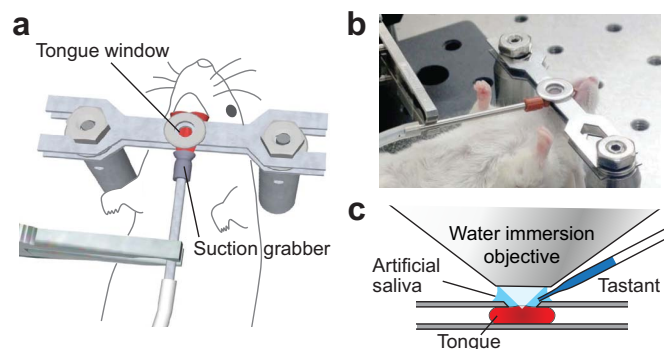


**Figure 1 | Setup for Intravital Tongue Imaging.** (a) Schematic. (b) Photograph. (c) Schematic of the setup for topical administration of aqueous tastant solution.

operation. Postmortem histological analysis showed no sign of cellular damage and macroscopic deformation of the tongue tissue (Supplementary Fig. S2). The tongue could be released reversibly by reducing the suction pressure. The externalized tongue was sandwiched between custom-designed stainless steel metal plates with gentle pressure (Supplementary Fig. S3). This arrangement stabilized tissue motion to the submicron level without compromising microvascular perfusion into the tissue. The top plate has an opening through which imaging was performed. The opening also allowed tastants to be administered topically onto the tongue (Fig. 1c). In the case of acute experiments, cyanoacrylate tissue adhesive can be used to hold the tongue by gluing the ventral surface to the bottom metal plate (Supplementary Fig. S1). For imaging, a water-immersion objective lens was used with artificial saliva as immersion solvent to maintain the physiological aqueous environment.

**Visualization of Taste Buds.** To understand endogenous multiphoton contrast in the dorsal surface of the tongue, we imaged unstained tongue with 100-fs excitation pulses at a central wavelength of 800 nm. The tongue exhibited bright multiphoton photoluminescence in the visible spectrum, which readily demarcated different types of papillary structures (yellow in Fig. 2a and Supplementary Fig. S4). The filiform papillae, cone-shaped

prominences covering most of the dorsum, were visualized by bright two-photon autofluorescence with broad emission spectra peaked at about 520 nm, mostly generated from keratin<sup>18</sup> in the keratinized stratified squamous epithelium (yellow in Figs. 2A). The extracellular collagen in the connective tissue around and underneath the taste buds in fungiform and circumvallate papillae generated second harmonic generation (SHG) signal, revealing a crater shape composed of fibrillar structure (blue in Fig. 2a and Supplementary Fig. S4). The spectrum of the SHG signal is centered at exactly the half of the excitation wavelength (i.e.  $\lambda_{em} = 400$  nm for  $\lambda_{ex} = 800$  nm). The SHG signal appeared only in the base of the taste bud but not under the entire epithelium. To visualize the taste cells in the taste buds, we loaded an anionic calcium indicator (calcium green-1 dextran) across the tongue dorsum. We placed a piece of dye-soaked paper tissue and applied uniform electrical pulses throughout the tongue surface using a tweezer-type electrode<sup>19</sup> (Supplementary Fig. S5). Using this method, we typically found nearly all taste buds ( $98.9 \pm 2.0\%$ ; 92 taste buds from 3 mice) stained over the entire image area ( $>7$  mm<sup>2</sup>). Interestingly, even though the calcium dye and electrical field were applied to the tongue surface homogeneously, the taste cells in taste buds were predominantly stained (Fig. 2b). We also observed the dye adsorbed onto the surface of the lingual epithelium, but the nonspecific dye was mostly washed away after rinsing with artificial saliva and almost completely removed by the time of imaging at 1–2 days after the staining. This selective intracellular loading is attributed to the high electrical conductivity of taste buds, compared to the surrounding, which results in high electrophoretic force into the taste cells. Blood vessels were stained by intravenously administered rhodamine-B dextran. In a 3D reconstructed view, individual taste cells have characteristic spindle shapes with their basolateral sides surrounded by the collagenous connective tissue (Fig. 2c and Supplementary Video S1). Projection of the microvilli towards the taste pores at the apical side was apparent<sup>20</sup>. A schematic of microanatomy of a taste bud is depicted in Fig. 2d (Supplementary Fig. S6).

**Functional Calcium Imaging of the Taste Cells.** Following the bulk loading of the calcium dye, we studied functional activity of taste cells in the taste buds (Fig. 3a). To quantify the tastant-evoked change in cellular calcium level, we took volumetric z-stacks of calcium

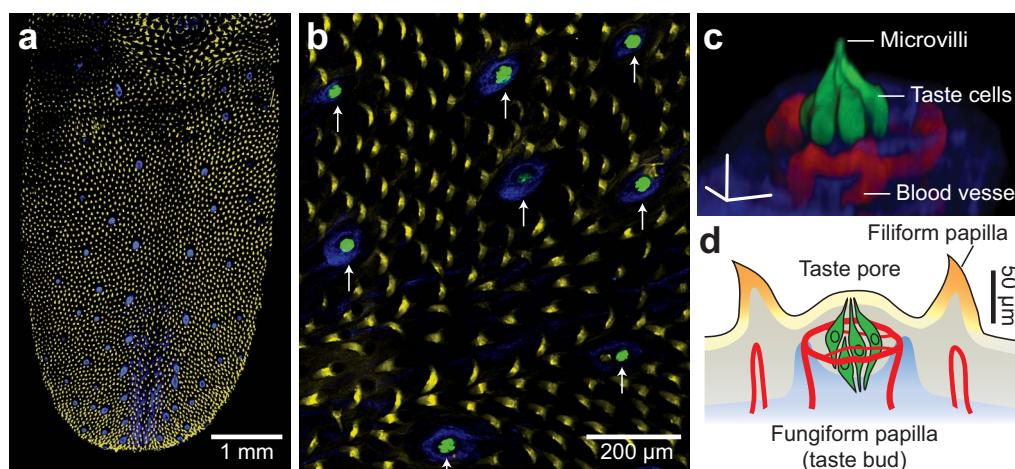


**Figure 2 | Microanatomy of the Tongue Mucosa.** (a) Comprehensive view of the tongue mucosa taken with two-photon excitation. Yellow, autofluorescence from keratinized lingual epithelial cells of filiform papillae. Blue, second-harmonic signal from collagen around individual taste buds. This label-free image comprises a mosaic of  $15 \times 19$  images, each acquired with an integration time of 2 s and an axial resolution of about  $10 \mu\text{m}$  using a  $10 \times 0.25$  NA objective lens. (b) Image after electrophoretic bulk loading of calcium-green dextran. The image was taken using a  $10 \times 0.25$  NA objective lens. Arrows indicate taste buds (green). (c) A 3D rendered view of a taste bud. The receptor cells (green) show typical spindle shape with their villi projecting towards the apical side. Red, blood vessels visualized by intravenous rhodamine-B dextran (70 kDa). The taste bud is surrounded by collagenous structure (blue). Scale bar,  $20 \times 20 \times 20 \mu\text{m}^3$ . (d) Schematic of a tongue mucosa in cross-sectional view.

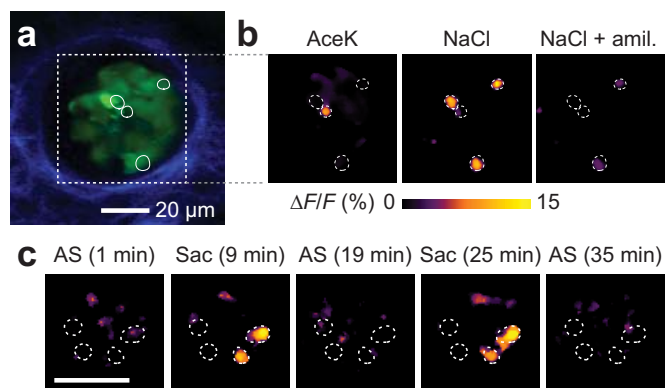


**Figure 3 | Functional Calcium Imaging of Intraoral Taste Sensing In Vivo.** (a) Baseline fluorescence of a taste bud loaded with calcium dye. (b) Calcium activity of taste cells in response to topically administered tastant stimuli: 40 mM acesulfame K, 180 mM NaCl, and 180 mM NaCl with 10  $\mu$ M amiloride, respectively. The pseudo-color map represents the calcium changes ( $\Delta F/F$ ) measured by fluorescence intensity. (c) Response to repeated stimuli of a sweet tastant: Na-saccharine, 40 mM. Artificial saliva (AS) and saccharine (Sac) were applied alternatively with a period of  $\sim$ 10 min. The calcium response map are shown.

fluorescence in a taste bud before and after tastant application. We noticed subtle motion artifact at the moment of applying tastant solution. To compensate this, we aligned two z-stack images by using intensity-based registration algorithm and computed the relative calcium-fluorescence change ( $\Delta F/F$ ) in each taste cells. This method allowed robust identification of the activated cells. When physiological amount of an artificial sweetener (40 mM acesulfame-K) or sodium salt (180 mM NaCl) was applied, each tastant elevated the intracellular calcium level by approximately 10%  $\Delta F/F$  in a specific, non-overlapping subpopulation of the taste cells (Fig. 3b). Epithelial sodium channel (ENaC) inhibitor, amiloride (10  $\mu$ M), inhibited the activity of salt-responsive cells (Fig. 3b). Repeated intermittent administration of sweet or salty tastant led to a reversible activation of the same taste cells, demonstrating robustness of the measurement (Fig. 3c and Supplementary Fig. S7). These results recapitulate previous findings of taste sensation obtained with *ex vivo* preparations, suggesting that “one cell, one taste” coding logic in the tongue is valid *in vivo* although further study may be warranted to prove the coding logic in the periphery.

**Vascular Physiology of the Tongue.** Intact vascular physiology is a hallmark of *in vivo* system. To study vascular perfusion near taste buds, we injected rhodamine-B dextran (70 kDa) intravenously as a blood tracer. Non-labeled red blood cells (RBCs) were identified as non-fluorescent dark objects flowing in blood vessels. The blood vessels were located about 80  $\mu$ m deep from the tissue surface, beneath the layer of filiform papillae (Fig. 2d). The imaging depth of two-photon microscopy was greater than 240  $\mu$ m, sufficient to visualize the epithelial vasculature comprehensively (Fig. 4a and Supplementary Fig. S8; Supplementary Video S2)<sup>22</sup>. Beneath each filiform papilla, there was a curly capillary without branching (Fig. 4a, marked by arrows). By contrast, each taste bud had complex vascular architecture composed of richly branched capillaries forming at least one closed loop around the taste cells (Fig. 4b). To understand microvascular perfusion in the taste bud, we quantified the flow velocity in each vascular segment by tracking RBC movement (Fig. 4c). Although the specific vascular architecture varied among the taste buds, several common features were identified as follows. A feeding arteriole bifurcates and anastomoses to form a closed loop. The multiple branches eventually drain into one or two venules with larger diameters (Fig. 4d, e). The capillaries in the taste buds are highly tortuous, much more than those elsewhere including

the brain cortex (Fig. 4f). We presume that the curly shape of the vessels in the tongue renders mechanical flexibility essential for dynamic tongue motion.

Next, we studied microvascular permeability in taste buds. When administered intravenously, small-molecular fluorescein (330 Da) rapidly permeated out of the luminal compartment and began to fill in the taste bud through paracellular diffusion (Fig. 4g). There was no noticeable diffusion of the dye to the apical side (Fig. 4h), indicating that the transport of the molecules is blocked by the tight junctions that separate the basolateral and the apical side. In the basolateral side, the extravasated dye reached the 25%, 50%, 75% and 90% levels of the maximum equilibrium concentration in 2.2, 3.6, 6.3 and 11 s, respectively, from the onset of the fluorescence signal (Fig. 4i). To verify this time delay is indeed due to molecular diffusion, we also tested dextran-conjugated fluorophores with different molecular weights of 4 kDa, 10 kDa, and 70 kDa, respectively. The diffusion time increased linearly with the hydrodynamic molecular size, in agreement with the Stokes-Einstein diffusion theory (Fig. 4j). No diffusion of 70 kDa molecules was observed. These results clearly show that small-sized molecules up to 10 kDa in blood circulation can reach the basolateral side of taste cells through diffusion within one minute. We note that all the molecules including fluorescein did not reach the apical taste pore where intraoral taste sensing takes place, conceivably due to tight junctions between taste cells.

**Intravascular Taste Sensation.** Having confirmed the molecular diffusion from blood circulation, we investigated the possibility of taste sensation from the pericellular blood vessels, a phenomenon called intravascular taste. Although phenomenological intravascular taste has long been known and was even used in the clinic to measure an arm-to-tongue circulation time, its mechanism has been only speculated, and it remains controversial whether taste cells mediate intravascular taste sensation<sup>23</sup>. To address this, we imaged the taste bud in real time while administering a tastant with an intravenous catheter via the retro-orbital route. An artificial sweetener, saccharine (183 Da), was chosen because it is known to generate intravascular taste sensation in humans and rodents. Rhodamine-B dextran (1% w/v, 70 kDa) was added to the tastant solution to visualize the arrival of the injected tastant to the pericellular capillary. Upon a bolus intravenous injection of the mixture of saccharin and dye, real-time fluorescence imaging indicated the arrival of these molecules to the vessel (Fig. 5a and Supplementary Fig. S9). The arrival time from the injection point was  $4.8 \pm 0.5$  s (Fig. 5b). The arrival of the molecules was followed by rapid calcium response in a subset of taste cells, consistent with apical taste stimulation. The intravascular taste sensation by taste cells is not limited to saccharin. Intravenous administration of a physiologic tastant, NaCl (500 mM) also elicited robust calcium response of subpopulation of taste cells (data not shown).

The latent time from the arrival of the molecule to the onset of the calcium response was  $1.4 \pm 0.9$  s, and the peak calcium response appeared  $16.0 \pm 1.4$  s after the onset (Fig. 5b). Our previous measurement of extravasation kinetics predicted that it would take about 10 s, or less, for the tastant to reach 90% concentration at the basolateral side of taste cells (Fig. 4j). We attributed the extra  $>6$  s of delay to the additional diffusion time taken for the molecules to diffuse through the tight junction and reach the apical sensing site—i.e. microvilli—of the taste cells. To verify this conjecture, we tested another sweet tastant molecule, sucrose, with a larger molecular size of 342 Da. Sucrose is small enough to extravasate and permeate through the basolateral space but supposed to be too large to cross the tight junction in the taste bud. As expected, sucrose did not elicit any response from the taste cells even at a near-maximal physiologic concentration of 500 mM in the blood circulation (Fig. 5c). This discrete size discrepancy further suggests that intravascular sensing occurs at the microvilli of the receptor cells.

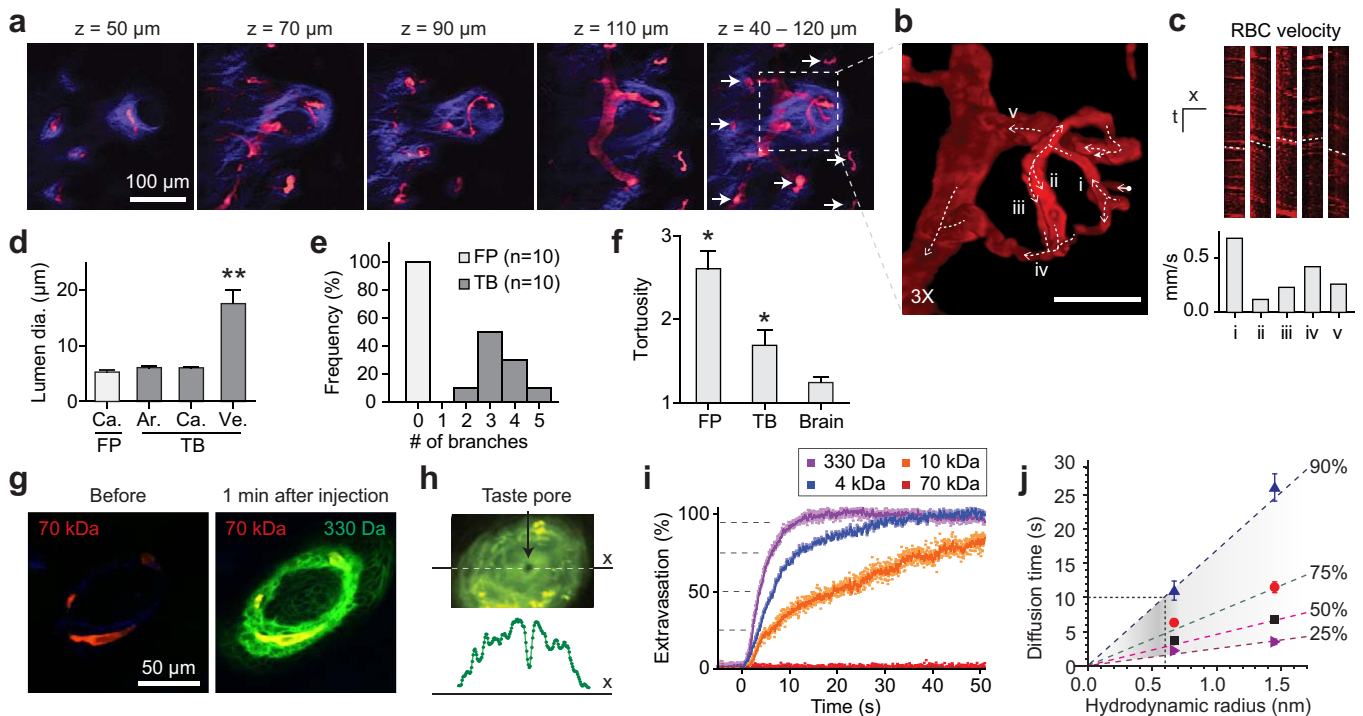


**Figure 4 | Vascular physiology of the tongue mucosa.** (a) Images at various depths from the surface. The right-most image is a projection of 40 z-stacks with an axial spacing of 2  $\mu\text{m}$ . Arrows indicate the capillaries beneath filiform papillae (FP). (b) A 3D rendered view of the vasculature in the taste bud (TB) demarcated by the dotted rectangle in (a). Arrows indicate the direction of blood flow. (c) Line-scan images and measured RBC velocity for the vessel segments, i–v, indicated in (b). (d) Measured lumen diameters in the capillaries (C), arteriole (A), and venule (V) in FP and TB. \*\*,  $P < 0.01$ . (e) Histogram of the number of capillary branches in each FP and TB in a fungiform papilla. (f) Measured vascular tortuosity in the tongue vs. brain cortex. Tortuosity is defined as the arc-chord ratio of vessel segments. \*,  $P < 0.05$ . (g) Fluorescence images of a blood vessel in a TB. Following administration of Rhodamine-B dextran (red, 70 kDa), images were taken before (left) and 1 min after (right) injection of fluorescein (green, 330 Da) via an intravascular catheter. (h) Image of a TB at the depth of the taste pore 5 min after the injection of fluorescein (green). The dark spot at the center corresponds to the location of taste pore. Bottom, intensity profile across a central axis (x, dotted line). (i) Transport kinetics of various dyes at the basolateral side of taste cells.  $t = 0$  corresponds to the arrival of dye at the pericellular blood vessel. (j) Relationship between the hydrodynamic radii of the injected molecules and the measured diffusion times (symbols) to reach specific concentration % levels relative to the steady-state maximum. Dashed lines, linear fit at various concentration levels. For molecules smaller than fluorescein, the diffusion time is expected to be shorter than 10 s (dotted lines). Scale bars, 50  $\mu\text{m}$  in (a), (b), and (g).

Another interesting kinetic feature we observed was that the calcium response attenuated rapidly within 1 min from its onset. This is more than one order of magnitude shorter than the plasma half-life of saccharine in circulation, which is  $\sim 10$  min in rodent<sup>24</sup>. We reasoned that the taste cells have sensory adaptation to intravascular saccharine as well as to intraoral tastant. To test this hypothesis, we monitored the calcium response of taste cells as saccharin was administered repeatedly at 10 min interval (Fig. 5d). Indeed our measurement showed that the peak response decreased drastically in the second injection of saccharine (Fig. 5e). At the third injection, the calcium response decreased down to the noise level (Fig. 5f). This result is in agreement with the previous observations of rapid attenuation in responsiveness with exposure to prolonged sweet taste<sup>21</sup>.

## Discussion

**Current Capabilities and Future Outlook.** We have described microscopic interrogation of the tongue in live animals for the first time to our knowledge. Using a video-rate two-photon microscopy, we demonstrated that our approach is well suited for studying physiologic dynamics, such as vascular perfusion, molecular diffusion, and functional mapping of taste cells, in the tongue. We further applied the technique to study intravascular taste sensation and revealed that small-molecular tastants (saccharine and sodium chloride) injected into the blood circulation elicits calcium activity of taste cells. Intravital microscopy of the tongue is expected to enable numerous studies previously difficult or not possible with *ex vivo*

preparations. We envision an optogenetic approach to control taste cells by introducing light-sensitive proteins into the cells<sup>25</sup>. Then, the imaging setup demonstrated here can be used to not only read their responses but also to activate or de-activate individual taste cells to study intercellular circuitry<sup>4</sup>. Furthermore, the penetration depth of multiphoton microscopy is sufficient to view the entire taste buds in mice and may be extended to measure the activities of the underlying gustatory nerves to study functional connectome and information processing between taste cells to the nerve fibers. This capability may help to address the grand debate in the field of taste: whether taste cell is a labeled-line system or combinatorial one<sup>26–28</sup>. It should be possible to perform tongue imaging in conjunction with conventional neurotechniques such as nerve electrophysiology and neuronal calcium imaging for comprehensive understanding of the taste transduction pathway (Supplementary Fig. S10). Microfluidic channels may be integrated into the tongue window to allow controlled delivery of multiple tastants at steady-state flow and enable studies with delicate combinations of different taste qualities. Furthermore, endoscopic probes can be employed to gain access to other regions in the oral cavity, such as posterior part of the tongue, buccal mucosa, and palates.

**Apical Sensing of Intravascular Taste.** Our study on intravascular taste provides direct evidence that it is the taste cells that mediate intravascular taste. Our data also suggest that the microvilli in the apical side of taste buds are the common active sensing site for

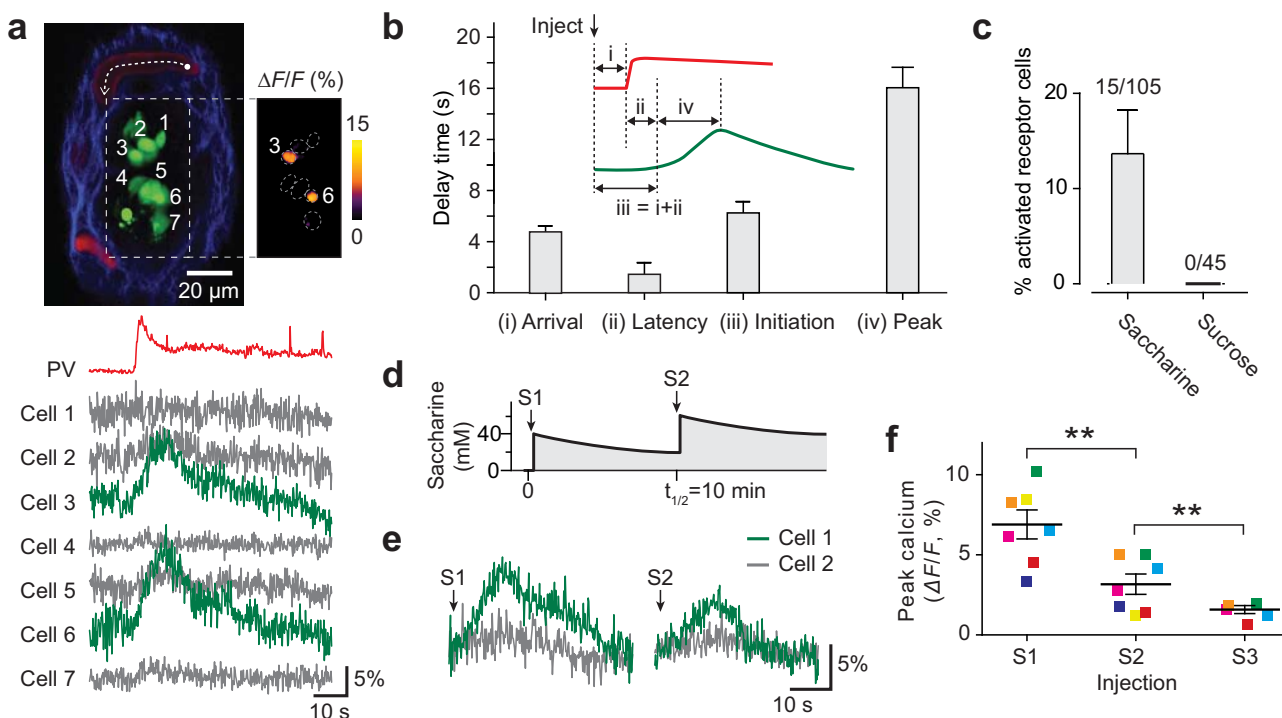


**Figure 5 | *In vivo* imaging of intravascular taste sensing.** (a) Taste cells in response to intravascular Na-saccharine. Left, taste cells (green) and pericellular blood vessel (PV) in a TB. Right, functional calcium image of the region in dashed box. Bottom, calcium traces of the receptor cells measured at 30 Hz and the trace of the injected dye (red) and tastant in the PV. Activated cells are highlighted in green. (b) Analysis of kinetic parameters from the calcium traces: Arrival (i) indicates the duration between the injection and arrival of the tastant to PV. Latency (ii) is a time delay between the arrival of tastant in PV and initiation of intracellular  $\text{Ca}^{2+}$ . (c) The % number of activated cells in response to intravascular saccharine (183 Da,  $n = 105$  cells in 13 TB's). None of the receptor cells ( $n = 45$  in 5 TB's) responded to intravascular sucrose (342 Da). (d–f) Adaptation to intravascular saccharine. (d) Intravascular concentration of saccharine estimated with first-order kinetics. S1 and S2 indicate the injection time points with an interval of 10 min. (e) Calcium traces of two representative taste cells in a TB. (f) The magnitude of peak calcium response to three injections (S1 to S3) with a 10-min interval. The decrease of response indicates an adaptation to the intravascular tastant. \*\*,  $P < 0.05$  by ANOVA test.

intravascular and intraoral taste. It has previously been questioned whether intravascular sensing should occur at the basolateral side of the taste cells because of the presence of the tight junctions that separate the apical and basolateral spaces. This was supported by experimental observations that amiloride (230 Da) administered topically did not affect the basolateral side and vice versa<sup>29</sup>. However, another study with electron micrographs suggested that tight junctions in taste buds are relatively leaky by showing diffusion of lanthanum (139 Da) across the tight junction<sup>30</sup>. In the present study, we provided quantitative evidence favoring apical sensing hypothesis by measuring the kinetics of cellular calcium activity in response to intravenously administered saccharin (183 Da) at real-time. The response of taste cells was significantly delayed compared to the estimated diffusion kinetics of saccharin to basolateral space, which can be reconciled by additional diffusion length to reach the apical site. We further verified that intravenous sucrose (342 Da), which is impermeable to the tight junction, failed to elicit activation of taste cells. Taken together, our results suggest that intravascular taste elicited by saccharine is sensed by microvilli at the apical side. It is known that some chemicals (e.g. salt, alcohol) from ingested foods are transported into blood circulation. Our result indicates that intravascular sensing of these chemicals may contribute to the taste sensing of certain foods and drinks.

**Other Applications in Peripheral Taste Research.** Beyond taste sensation, intravital tongue imaging is expected to provide a wide range of applications, particularly for pathogenesis and homeostatic maintenance, by allowing longitudinal observation of cellular dynamics over prolonged period of time. The lingual keratinized epithelial cells constituting the filiform papillae are one of the most

rapidly regenerating cells in the body, with a typical turn over time of 10 days in human. Their rapid proliferation is closely associated with the genesis of squamous cell carcinoma<sup>31</sup> and oral mucositis after cancer therapy<sup>32</sup>. Observing cellular dynamics during the disease progression and therapeutic interventions would facilitate deeper understanding on cellular mechanisms. Moreover, dynamic repopulation of the taste cells, and their renewed connectivity to the afferent nerve fibers should offer an exciting model to study highly orchestrated cellular maintenance and plasticity<sup>33,34</sup>. Structural and functional mapping of vascular network in the taste bud may also be useful to elucidate the functional role of vascular perfusion in peripheral taste sensation and to measure the potential spatiotemporal correlation (i.e. neurovascular coupling) between neuronal activity and vascular perfusion in the tongue.

## Methods

**Mouse preparation.** All experiments were conducted with 7- to 10-week-old male BALB/c mice (Jackson Laboratory). The mice were anesthetized by intraperitoneal injection of ketamine (90 mg/kg; Pfizer) and xylazine (9 mg/kg; Bayer Healthcare) in phosphate buffered saline (PBS; Life Technologies). The tongue of an anesthetized mouse was gently pulled out with a rubber-tip forceps and stabilized either by holding with a suction grabber with a pressure of 25 mmHg or by gluing onto a bottom metal plate with cyanoacrylate tissue adhesive (~2  $\mu\text{l}$ ) (see Supplementary Fig. S1). A top metal plate was then placed onto the tongue with gentle pressure, monitoring the apparent color of the tongue by naked eyes to ensure normal perfusion. Under intravital microscopy, normal blood perfusion was readily confirmed by observing the flow speed of intravascular dye. During the mounting procedure, the tongue was kept wet by applying artificial saliva (2 mM NaCl, 5 mM KCl, 3 mM  $\text{NaHCO}_3$ , 3 mM  $\text{KHCO}_3$ , 0.25 mM  $\text{CaCl}_2$ , 0.25 mM  $\text{MgCl}_2$ , 0.12 mM  $\text{K}_2\text{HPO}_4$ , 0.12 mM  $\text{KH}_2\text{PO}_4$ , 1.8 mM HCl, pH7). All animal experiments were performed in compliance with institutional guidelines and approved by the committees on research animal care and use at the Massachusetts General Hospital and Harvard Medical School.



**Two-photon microscopy and Spectroscopy.** A home-built two-photon microscope with a Ti:Sapphire laser (MaiTai DeepSee, Newport) was used for imaging. A laser scanner comprised a rotating polygon mirror ( $x$ -axis) and a galvano-scanner mirror ( $y$ -axis), generating a frame rate of 30 Hz. The laser power was adjusted by using a rotatable half-wave plate coupled with a polarizing beam splitter. A 1.0 NA water-immersion objective lens (Olympus) was used for all experiments, if not stated otherwise. The system had three detection channels, each consisting of a photomultiplier tube and dichroic filters:  $405 \pm 10$  nm for blue second harmonic generation signal,  $525 \pm 25$  nm for green autofluorescence, and  $600 \pm 50$  nm for red fluorescence. For the spectral analysis of two-photon luminescence, the light emitted from the tissue was coupled to a multimode optical fiber (FT1500EMT, Thorlabs) and analyzed by a spectroscope (Dongwoo Optron) with an electron-multiplying CCD (Newport).

**Vascular imaging.** After anesthesia, the mouse was intravenously injected with rhodamine-B dextran (70 kDa) or TRITC-dextran (2 MDa, TdB Consultancy AB) dissolved in phosphate-buffered saline (100  $\mu$ l, 2.5% w/v).

**Electrophoretic staining of taste cells.** After anesthesia, the mouse was placed in the supine position, and the tongue was gently externalized by using the rubber-tipped forceps. A piece of paper tissue ( $\sim 4$  by 4 mm<sup>2</sup>) soaked with calcium green dextran (5% w/v) was placed on the anterior dorsal surface of the tongue and then electric pulses (5 Vpp, 2 Hz, pulse width: 100 ms, duration: 10 s) from a function generator were applied through a tweezer-type electrode (Tweezertrode, Harvard Apparatus) for electrophoresis (Supplementary Fig. S5). The stained tongue was rinsed with artificial saliva several times to remove nonspecifically bound dyes in the epithelium. Imaging experiments were conducted 1 to 2 days after the calcium loading procedure.

**Apical taste stimulation.** For apical taste stimulation, tastant dissolved in artificial saliva was applied to the dorsal surface of the tongue (See Fig. 1c). For calcium imaging,  $z$ -stack images (2  $\mu$ m interval, 2 s per image, 30 to 40 images) of a taste bud are acquired as the immersion solution was changed between 100% artificial saliva and the tastant solution (See Fig. 2c–e).

**Intravascular taste.** For measuring the response of taste cells to intravascular tastant (saccharine), a movie of fluorescence images of taste cells loaded with calcium green dextran was acquired at 30 frames per second, during and after the retro-orbital injection of the tastant (50  $\mu$ l in PBS) into the bloodstream. For adaptation experiment (Fig. 5d–f), the same amount of tastant was injected multiple times with a 10 min interval.

**Histology.** After euthanasia, the tongue was excised from the mouse and fixed in 4% formalin for 48 hours or longer. The tongue was frozen-sectioned with 5  $\mu$ m thickness and stained with hematoxylin and eosin (H&E). Optical images of the slides were obtained by using a bright-field microscope (IX71, Olympus) with a 4  $\times$  objective lens.

**Data analysis.** Image processing plugins for Fiji (ImageJ, NIH) and Matlab (Mathworks) were used for image registration, stitching, arithmetic operation, filtering and quantification. The calcium activity of taste cells was measured from time-lapse  $z$ -stack images acquired, typically, over the middle portion of the taste bud where cell bodies are clearly distinguished. We confirmed if the adjacent planes (2–4  $\mu$ m above or below) exhibited consistent activity patterns to validate the measurement. GraphPad Prism software was used for statistical analysis. Data are expressed as mean  $\pm$  standard error. Statistical differences were analyzed by  $t$ -test or ANOVA where indicated and  $p$ -value lower than 0.05 was considered to be statistically significant.

- Liman, E. R., Zhang, Y. V. & Montell, C. Peripheral Coding of Taste. *Neuron* **81**, 984–1000 (2014).
- Chaudhari, N. & Roper, S. D. The cell biology of taste. *J. Cell. Biol.* **190**, 285–296 (2010).
- Chaudhari, N. Synaptic communication and signal processing among sensory cells in taste buds. *J. Physiol.* **592**, 3387–3392 (2014).
- Roper, S. D. Taste buds as peripheral chemosensory processors. in *Semin. Cell. Dev. Biol.* **24**, 71–79 (2013).
- Fortis-Santiago, Y., Rodwin, B. A., Neseliler, S., Piette, C. E. & Katz, D. B. State dependence of olfactory perception as a function of taste cortical inactivation. *Nat. Neurosci.* **13**, 158–159 (2010).
- Kawai, K., Sugimoto, K., Nakashima, K., Miura, H. & Ninomiya, Y. Leptin as a modulator of sweet taste sensitivities in mice. *Proc. Natl. Acad. Sci. U.S.A.* **97**, 11044–11049 (2000).
- de Araujo, I. E. *et al.* Food reward in the absence of taste receptor signaling. *Neuron* **57**, 930–941 (2008).
- Scanziani, M. & Hausser, M. Electrophysiology in the age of light. *Nature* **461**, 930–939 (2009).
- Grienberger, C. & Konnerth, A. Imaging calcium in neurons. *Neuron* **73**, 862–885 (2012).
- Chen, X., Gabitto, M., Peng, Y., Ryba, N. J. & Zuker, C. S. A gustotopic map of taste qualities in the mammalian brain. *Science* **333**, 1262–1266 (2011).
- Dando, R., Dvoryanchikov, G., Pereira, E., Chaudhari, N. & Roper, S. D. Adenosine enhances sweet taste through A2B receptors in the taste bud. *J. Neurosci.* **32**, 322–330 (2012).

- Oka, Y., Butnaru, M., von Buchholtz, L., Ryba, N. J. & Zuker, C. S. High salt recruits aversive taste pathways. *Nature* **494**, 472–475 (2013).
- Andermann, M. L. *et al.* Chronic cellular imaging of entire cortical columns in awake mice using microprisms. *Neuron* **80**, 900–913 (2013).
- Farrar, M. J. *et al.* Chronic in vivo imaging in the mouse spinal cord using an implanted chamber. *Nat. Methods* **9**, 297–302 (2012).
- Kim, J. K. *et al.* Fabrication and operation of GRIN probes for in vivo fluorescence cellular imaging of internal organs in small animals. *Nat. protoc.* **7**, 1456–1469 (2012).
- Looney, M. R. *et al.* Stabilized imaging of immune surveillance in the mouse lung. *Nat. Methods* **8**, 91–96 (2011).
- Ritsma, L. *et al.* Intravital microscopy through an abdominal imaging window reveals a pre-micrometastasis stage during liver metastasis. *Sci. Transl. Med.* **4**, 158ra145 (2012).
- Zheng, W., Wu, Y., Li, D. & Qu, J. Y. Autofluorescence of epithelial tissue: single-photon versus two-photon excitation. *J. Biomed. Opt.* **13**, 054010–054018 (2008).
- Caicedo, A., Jafri, M. S. & Roper, S. D. In situ Ca<sup>2+</sup> imaging reveals neurotransmitter receptors for glutamate in taste receptor cells. *J. Neurosci.* **20**, 7978–7985 (2000).
- Farbman, A. I. Electron microscope study of the developing taste bud in rat fungiform papilla. *Dev. Biol.* **11**, 110–135 (1965).
- Nelson, G. *et al.* Mammalian sweet taste receptors. *Cell* **106**, 381–390 (2001).
- Hua, T.-E., Yang, T.-L., Yang, W.-C., Liu, K.-J. & Tang, S.-C. 3-D neurohistology of transparent tongue in health and injury with optical clearing. *Front. Neuroanat.* **7**, 36 (2013).
- Bradley, R. M. Electrophysiological investigations of intravascular taste using perfused rat tongue. *Am. J. Physiol.* **224**, 300–304 (1973).
- Sweatman, T. W. & Renwick, A. G. The tissue distribution and pharmacokinetics of saccharin in the rat. *Toxicol. Appl. Pharmacol.* **55**, 18–31 (1980).
- Yizhar, O., Fenno, L. E., Davidson, T. J., Mogri, M. & Deisseroth, K. Optogenetics in neural systems. *Neuron* **71**, 9–34 (2011).
- Horton, N. G. *et al.* In vivo three-photon microscopy of subcortical structures within an intact mouse brain. *Nat. Photonics* **7**, 205–209 (2013).
- Chaudhari, N. & Roper, S. D. The cell biology of taste. *J. Cell Biol.* **190**, 285–296 (2010).
- Frank, M. E., Lundy Jr, R. F. & Contreras, R. J. Cracking taste codes by tapping into sensory neuron impulse traffic. *Prog. Neurobiol.* **86**, 245–263 (2008).
- Mierson, S., Olson, M. M. & Tietz, A. Basolateral amiloride-sensitive Na<sup>+</sup> transport pathway in rat tongue epithelium. *J. Neurophysiol.* **76**, 1297–1309 (1996).
- Holland, V., Zampighi, G. & Simon, S. Tight junctions in taste buds: possible role in perception of intravascular gustatory stimuli. *Chem. Senses* **16**, 69–79 (1991).
- Tanaka, T. *et al.* Identification of stem cells that maintain and regenerate lingual keratinized epithelial cells. *Nat. Cell Biol.* **15**, 511–518 (2013).
- Sonis, S. T. The pathobiology of mucositis. *Nat. Rev. Cancer* **4**, 277–284 (2004).
- Yarmolinsky, D. A., Zuker, C. S. & Ryba, N. J. Common sense about taste: from mammals to insects. *Cell* **139**, 234–244 (2009).
- Zhang, Y. V., Raghuvanshi, R. P., Shen, W. L. & Montell, C. Food experience-induced taste desensitization modulated by the *Drosophila* TRPL channel. *Nat. Neurosci.* **16**, 1468–1476 (2013).

## Acknowledgments

We thank K.B. Lee, H. Koo, and S.J.J. Kwok in the Wellman Center for Photomedicine for helpful discussions and J. M. Bekker in Australian National University for comments. This work was in part funded by the U.S. National Institutes of Health (P41EB015903, U54CA143837) and a Postdoctoral Fellowship from the National Research Foundation of Korea (NRF-2013R1A6A3A03060958).

## Author contributions

M.C. and S.H.Y. designed the research. M.C. and W.M.L. developed the imaging system. M.C. performed experiments and analyzed data. M.C., W.M.L. and S.H.Y. discussed the results. M.C. and S.H.Y. wrote the manuscript.

## Additional information

Supplementary information accompanies this paper at <http://www.nature.com/scientificreports>

**Competing financial interests:** The authors declare no competing financial interests.

**How to cite this article:** Choi, M., Lee, W.M. & Yun, S.H. Intravital Microscopic Interrogation of Peripheral Taste Sensation. *Sci. Rep.* **5**, 8661; DOI:10.1038/srep08661 (2015).



This work is licensed under a Creative Commons Attribution-NonCommercial-NoDerivs 4.0 International License. The images or other third party material in this article are included in the article's Creative Commons license, unless indicated otherwise in the credit line; if the material is not included under the Creative Commons license, users will need to obtain permission from the license holder in order to reproduce the material. To view a copy of this license, visit <http://creativecommons.org/licenses/by-nc-nd/4.0/>